

Article

Tribocorrosive Study of New and In Vivo Exposed Nickel Titanium and Stainless Steel Orthodontic Archwires

Tadeja Kosec ^{1,*}, Petra Močnik ¹, Uroš Mezeg ², Andraž Legat ¹, Maja Ovsenik ², Monika Jenko ³, John T. Grant ⁴ and Jasmina Primožič ²

¹ Slovenian National Building and Civil Engineering Institute, Dimičeva 12, 1000 Ljubljana, Slovenia; petra.mocnik@zag.si (P.M.); andraz.legat@zag.si (A.L.)

² Medical Faculty, University of Ljubljana, Vrazov trg 2, 1000 Ljubljana, Slovenia; beli.medved@telemach.net (U.M.); maja.ovsenik@mf.uni-lj.si (M.O.); jasmnaprimozic@gmail.com (J.P.)

³ Institute for Metals and Technology, Lepi pot 11, 1000 Ljubljana, Slovenia; monika.jenko@imt.si

⁴ Research Institute, University of Dayton, 300 College Park, Dayton, OH 45469, USA; grantjt@gmail.com

* Correspondence: Tadeja.kosec@zag.si; Tel.: +386-1-280-4547

Received: 6 February 2020; Accepted: 29 February 2020; Published: 3 March 2020



Abstract: The surface, corrosion and wear properties of new and in vivo exposed nickel titanium (NiTi) and stainless steel (SS) archwires used in orthodontic treatment were investigated. Electrochemical and tribo-electrochemical tests in artificial saliva were performed in order to define corrosion properties and to estimate wear rate of new and in vivo exposed NiTi and SS archwires. The surface chemical analysis of the passive film on the NiTi and SS archwires before and after tribocorrosion tests was performed by Auger Electron Spectroscopy (AES). In vivo exposed NiTi and SS archwires had better electrochemical properties than new archwires due to the protective nature of oral deposits. Total wear and coefficients of friction were higher among in vivo exposed archwires and higher in NiTi archwires in comparison to SS archwires. The estimated thickness of the TiO₂ passive film on as-received NiTi is 8 nm, while the passive Cr₂O₃ film on as-received SS is just 1–2 nm. On in vivo exposed NiTi archwire, a 60–80 nm thick organic film/dental plaque was observed, and on SS, it was thinner, at about 60 nm. This research shows the importance of combining AES with electrochemical testing, to characterize tribocorrosive properties of NiTi and SS orthodontic archwires.

Keywords: NiTi; stainless steel; dental alloy; corrosion; tribocorrosion; surface properties; Auger Electron Spectroscopy

1. Introduction

In orthodontic treatment, the friction force is influenced by mechanical (surface roughness and type of ligatures in the archwire system) and biological factors [1–3]. Biological factors are saliva [4], corrosion [5] and debris [1,6]. The surface properties of archwires and their possible intraoral degradation might affect the friction force and hence the effectiveness of orthodontic treatment.

Friction force among different brackets and archwires can cause up to a 50% reduction in the force necessary for tooth movement [3], resulting in a significant slowdown of tooth movement. If the friction force is reduced, the time required for orthodontic treatment can be shortened. Manufacturers of orthodontic brackets endeavor to reduce friction force by developing new bracket systems and improving the properties of archwires [7].

Previous studies on dental archwires are divided into four distinctive areas of research: (i) corrosion of dental archwires [8–10]; (ii) biocompatibility and nickel release from NiTi alloys [11–15]; (iii) versatile surface treatments to tailor properties, such as oxidation procedures [9,16]; and (iv)

different coatings on dental archwires that lower surface roughness and coefficient of friction [17]. Furthermore, coatings on NiTi include physical or chemical vapour deposition, ion implantation and thermal treatments leading to deterioration of NiTi properties, causing the diffusion of NiO into the TiO₂ phase [18]. Recent investigations have been conducted on the advancements of antimicrobial dental materials by using synthetic polymers from polyaniline or poly lactic-co-glycolic acid, incorporating different nanoparticles, due to its excellent biocompatibility and biodegradability [19,20].

However, in the oral cavity, orthodontic appliances are subjected to both chemical and mechanical wear, which may influence their performance. Clinicians can choose the type of bracket, ligature/clip, or archwire type, and with these, they can influence the friction force; on the other hand, patient controls the amount of accumulated debris. The impact of saliva on the friction was reported in the examination of surface and archwire material after intraoral long-term exposure [6]. Previously, friction was studied on as-received archwires and brackets, and either in vitro [21] or in vivo aged ones [22]. Intraoral exposure of rectangular stainless-steel (SS) archwires showed higher debris accumulation, correlated to friction as well [1,2]. In these studies, only short-term exposures were conducted [1,2]. Intraoral exposure of orthodontic material can take several weeks or months, which can affect surface properties and changes in friction manners. The friction forces and their relation to wear and accumulation of the debris in long-term in vivo experiments are of great importance [6].

Mezeg [23] reported that, on in vivo NiTi exposed archwires, the thick film of organic origin contains mainly C and O, with traces of P, Na, K and Cl. FTIR results showed the presence of the minerals apatite Ca₅(PO₄)₃(F,Cl,OH), calcite (CaCO₃) and halite (NaCl), as well as sylvite (KCl). In vivo exposed SS archwires were coated also by a thick film of organic origin. Semi-quantitative EDS showed mainly C and O and traces of Ca, P, Na, K and Cl. FTIR analysis confirmed the presence of Ca-apatite, halite and sylvite [23].

Ovsenik et al. reported [24] the results of surface analysis, using AES and XPS of new and in vivo exposed NiTi and SS archwires. The thin oxide films on new NiTi archwire were mainly 4 nm thick TiO₂. In vivo exposed NiTi archwire was 80 nm thick, with surface film of organic origin, namely dental plaque. A very thin (1–2 nm) Cr₂O₃ layer forms on a new SS archwire, while on in vivo exposed SS, a thick (60–80 nm) organic layer was analyzed.

Tribocorrosion of dental archwires is relatively difficult to study due to the nature of the experiment which foresees the use of a linear reciprocating tribometer. Furthermore, in vitro studies have been made on pin on disc tribometers, primarily on SS, in bio-simulated fluids and on disc plates [25–28], but there has been no report in the literature on tribocorrosion of both new and in vivo exposed NiTi and SS orthodontic archwires.

The aim of the study for clinical relevance is to study the effect of surface properties of the new and in vivo exposed NiTi and SS archwires with accumulated plaque on the coefficient of friction. The latest can then affect the orthodontic treatment.

However, on the phenomenological part, the aim of the study is to define possible differences of new and in vivo exposed archwires, their different electrochemical and wear properties, as well as the thickness and type of oxide films and plaque on the surfaces of the archwires.

2. Materials and Methods

2.1. Samples

Two types of orthodontic archwires were explored: a nickel-titanium (Neo Sentalloy; 51% Ni, Ti balance) rectangular 0.457 × 0.635 mm archwire (referred to as the “NiTi archwire”), and a stainless-steel (AISI 304 alloy; 69.5% Fe, 18.5% Cr, 9% Ni, 1% Mn, 0.75% Co, Si, C, P and S less than 1%) rectangular 0.483 × 0.635 mm archwire (referred to as the “SS archwire”), both from the same manufacturer (Dentsply GAC, NY, NY, USA). The concentrations are in wt.%.

Both new and in vivo exposed orthodontic archwires, which were exposed to the conditions in patients’ mouths for at least two months, were analyzed. Values of surface roughness and Vickers

hardness of the investigated archwires are given in Table 1. Vickers hardness tests were performed, using Frank Finotest 38542 equipment, Weinheim-Birkenau, Germany) applying a load of 9.8 N to cross-sections of the samples which had been prepared for the micro-structural metallographic investigation. Roughness was measured by profilometer (Taylor Hobson, Surtronic 25, Cedex, France, 2010). The samples for the electrochemical and tribo-electrochemical tests were obtained by cutting approximately 30 mm of each NiTi and SS archwire, either new or in vivo exposed, along its straight part. Archwires were ultrasonically cleaned by 1 min immersion in ethanol.

Table 1. Vickers hardness values (VHV) and roughness (Ra in nm) on NiTi and SS samples.

Archwire	Vickers Hardness	Ra
New NiTi archwire	376 ± 50	115 ± 5
In vivo exposed NiTi archwire		105 ± 3
New SS archwire	597 ± 20	15 ± 2
In vivo exposed SS archwire		14 ± 2

2.2. Electrochemical Measurements

Tests were performed at 37 °C in an artificial saliva, pH = 6.5, containing various halides, phosphate, carbonate salts and citric acid [29,30].

Corrosion cell had a volume of 0.8 L and the working area was 1.0 cm². An external heating unit was used to keep electrolyte at 37 °C. A floating version Autolab PGStat 100 expanded by Nova software 1.10 was used for analysis (Autolab, Utrecht, the Netherlands).

First, open-circuit potential (OCP) was measured for 2 h. Then, the cyclic polarization measurements were conducted. The measurement started at −0.25 V vs. OCP in the anodic direction up to +1.4 V, 1 mV/s. At 1.4 V vs. E_{ref} , or when a current density was 0.01 mA/cm², the scan was reversed. Potentials are reported with respect to the saturated calomel electrode (SCE) scale, unless stated otherwise. Minimum three measurements were conducted in electrochemical and two measurements in triboelectrochemical, in order to identify and minimize errors in the electrochemical testing [31]. The number of tested in vivo exposed archwires was limited due to specific nature of the representativity of the specimens.

2.3. Wear Measurements

A reciprocal tribometer (Tribotechnic, 2009, Clichy, France) using a 6 mm diameter Al₂O₃ ball as a counter-body was used for wear measurements. The archwires were glued onto a glass fiber resin with the electrical contact attached. Figure 1 shows the experimental setup. The normal load was 1 N, presenting contact pressure of 740–751 MPa (SS archwire) and 470–496 MPa (NiTi archwire). The average sliding speed was 0.33 mm/s, and the length of the wear track was 2000 mm, with the total duration of wear being 6060 s. The tribo-electrochemical cell was made of PEEK (polyether ether ketone), with the archwire as a working electrode (Figure 1b), a platinum counter-electrode and an Ag/AgCl reference electrode. The wear measurements were conducted at room temperature, since setup design did not enable testing at elevated temperatures.

Wear mechanisms were studied. Wear rate was determined by comparing the wear in deionized water, as a noncorrosive environment, and in corrosive artificial saliva. Repassivation time was determined from the E_{corr} vs. time curve after the end of rubbing of the samples, and was defined as the time when the sample reached a stable corrosion potential.

The wear volume was estimated, using a potentiostatic method, by analyzing the current at constant applied potential. The volume loss due to tribocorrosion (in mm³) was calculated, considering Faraday's law [32]:

$$V = (Q \times M) / (\rho \times n \times F) \quad (1)$$

where Q (C, As) is the measured charge, calculated by integrating the current measured during the experiment over time; M (g/mol) is the atomic weight of the alloy; ρ (g/mm³) is the density of the material; n is the valence of the element ($n = 2$ was used in this study); and F is Faraday's constant (96490 C/mol).

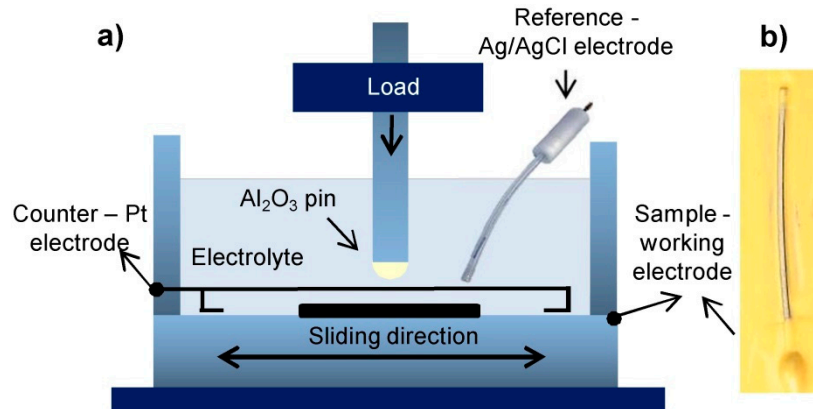


Figure 1. Experimental setup for the tribo-electrochemical investigation (a); a prepared working electrode from a section of the archwire for the tribo-electrochemical measurements (b).

During the tribo-electrochemical experiments (E vs. t and I vs. t), the friction force and the coefficient of friction (COF) were measured against time.

2.4. Surface Analysis

Auger Electron Spectroscopy (AES, Thermo Scientific VG Microlab 310-F spectrometer, East Grinstead UK) was used for the surface chemistry and depth profiles of surface films on new and in vivo exposed NiTi and SS archwires before and after tribocorrosion tests. Thickogram procedure was used for estimation of the thinnest oxide layers, Cr_2O_3 on new SS [33,34]. The accelerating voltage range was 0.5 to 25 kV. An energy resolution of the analyzer was 0.5%.

AES depth profiling was performed by argon-ion sputtering at 3 keV, at an angle of incidence of 0° and Auger emission angle of 30° , and scanning the ion beam over a $2\text{ mm} \times 2\text{ mm}$ area, allowing 0.7 nm/min sputter rate. AES spectra were acquired, using Avantage 3.41v data-acquisition and data-processing software supplied by Thermo Scientific. CasaXPS software, Version 2.3.22 (www.casaxps.com) was used for detailed data processing.

3. Results

3.1. Electrochemical Properties

The electrochemical properties of the new and in vivo exposed NiTi and SS archwires were studied by measuring cyclic potentiodynamic (CP) curves. The results are reported in Table 2 and Figure 2.

Table 2. Electrochemical properties derived from cyclic polarization curves, presented in Figure 2.

Archwire	E_{corr} (V)	j_{corr} (nA/cm ²)	E_b (V)	E_{rp} (V)
New NiTi archwire	-0.306	19	1.08	
In vivo exposed NiTi archwire	-0.193	10	1.17	
New SS archwire	-0.234	106	0.340	0.083
In vivo exposed SS archwire	-0.194	27	0.748	0.217

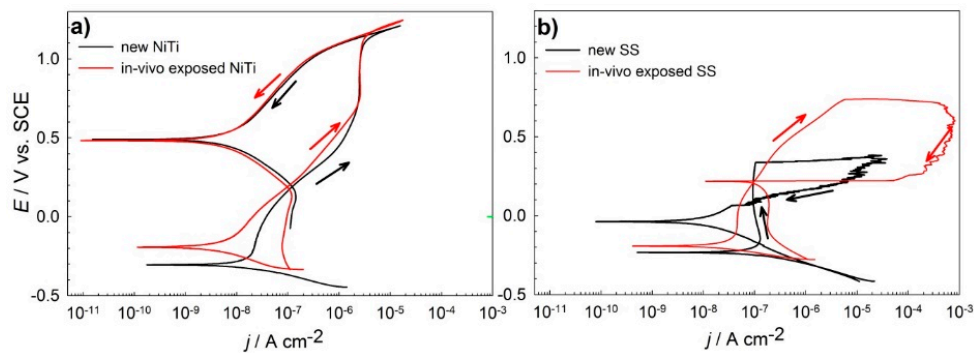


Figure 2. Cyclic potentiodynamic curves for the new (black line) and in vivo exposed (red line) (a) NiTi archwires and (b) SS archwires in artificial saliva at a scan rate of 1 mV/s.

The shape of CP curves for NiTi showed negative hysteresis. The corrosion current density for the new NiTi archwire (Figure 2b) was 19 nA/cm^2 , and for the in vivo exposed archwire, it was lower, at 10 nA/cm^2 . In the forward scan, low and slowly increasing current density was measured, showing passive behavior. The forward passive current was lower for in vivo exposed NiTi archwire when compared to the new one. The E_{corr} for in vivo exposed NiTi was slightly more positive (-0.193 V), with the results shown in Table 2. The rapid increase in the current density due to trans-passivity was at 1.08 and 1.17 V for the new and in vivo exposed archwire, respectively. The reverse scans showed currents which were smaller than those obtained in the forward scan. The results revealed that, under the studied conditions, the NiTi archwires could successfully re-passivate.

In the case of the new SS archwire (Figure 2b, black line), the corrosion potential was more negative (-0.234 V) than for the in vivo exposed SS archwire (-0.194 V). Moreover, j_{corr} for the new SS archwire was 106 nA/cm^2 , and it was higher than for the in vivo exposed SS archwire (Figure 2b, red line), 27 nA/cm^2 . The breakdown potential was low, at 0.34 and 0.7 V for the new and in vivo exposed SS archwires, respectively. Scanning in the reverse direction showed a positive hysteresis for both archwires, indicating the susceptibility to pitting or crevice corrosion of the SS archwires.

3.2. Tribo-Electrochemical and Surface Properties

The results of the tribocorrosion experiments on both the new and the in vivo exposed NiTi archwires revealed a decrease in the corrosion potentials during sliding (Figure 3a). The variation in the corrosion potential (E_{corr}) during sliding was higher for the in vivo exposed NiTi archwire. The re-passivation time was estimated from tribocorrosion experiments, as the time when the potential returns close to the value before sliding. At a normal load of 1 N, the re-passivation time was estimated to be 100 s for the new NiTi archwire and 90 s for the in vivo exposed NiTi archwire.

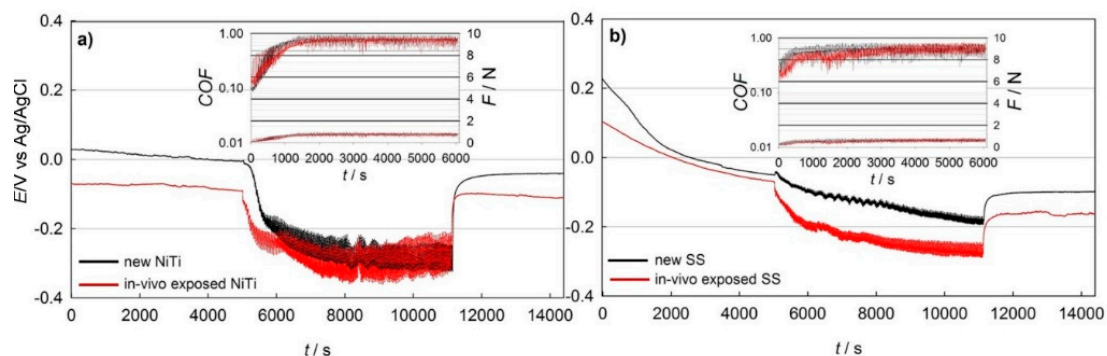


Figure 3. Corrosion potentials and coefficients of friction vs. time during sliding for the new (black line) and in vivo exposed (red line) (a) NiTi archwires and (b) SS archwires against an Al_2O_3 ball in artificial saliva.

Figure 3b shows the decrease in the corrosion potentials for the new and in vivo exposed SS archwires in artificial saliva during sliding. After the start of sliding, the potential decreased less ($\Delta \approx 100$ mV) and more slowly when compared to the NiTi archwires. The repassivation time for the SS archwires was 120 s for the new SS archwire, and 160 s for the in vivo exposed SS archwire.

The insets in Figure 3 show the coefficients of friction, COF, for the NiTi and SS archwires tested in artificial saliva, at a slow sliding speed of 0.33 mm/s and a 1 N normal load. The COF curves show that, in the case of the new NiTi archwire (Figure 3a, black line), the steady state COF at a 1 N load was 0.75, whereas in the case of the in vivo exposed NiTi archwire (Figure 3a, red line), the COF was slightly higher, i.e., 0.80. The observed COF was lower (0.60) for the SS archwires than for the NiTi archwires. However, the run-in period was shorter in the case of the new SS archwires in comparison to the in vivo exposed SS archwire.

The total wear contributions for the new and in vivo exposed archwires were calculated, and the observed wear rates are presented in Figure 4.

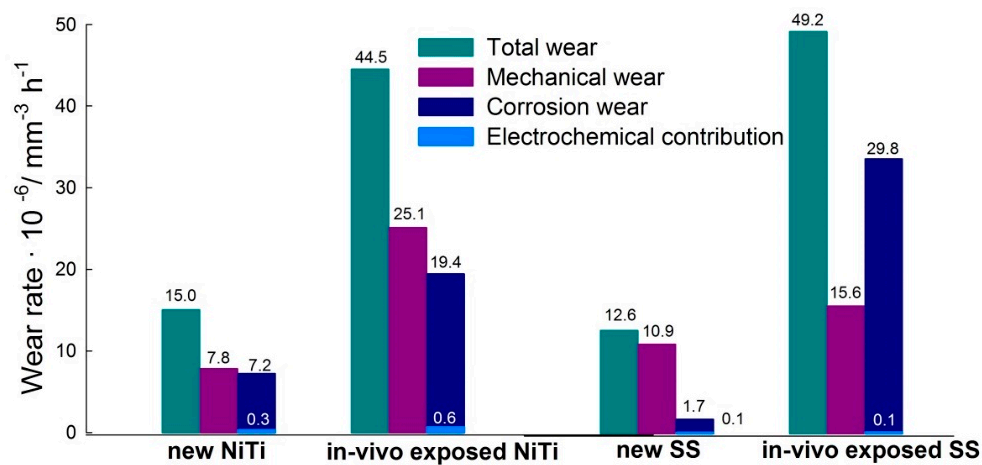


Figure 4. The contribution of mechanical and corrosion wear to total wear for the new and in vivo NiTi and SS archwires.

The total wear of the new NiTi archwire was higher than that of the new SS archwire, 15.0 vs. 12.6 mm³/h, respectively. The mechanical contribution to the total wear, estimated from the tests in noncorrosive media, was 52% and 87% for the new NiTi and new SS archwire, respectively. In the tribo-electrochemical experiments, the corrosion-wear component was as high as 48% for the new NiTi archwire, whereas in the case of the new SS archwire, it was only 13%. The loss of material due to the corrosion process alone was calculated from the electrochemical parameters, and amounted to relatively small values of about 0.03×10^{-5} mm³/h for the new NiTi archwire, and 0.009×10^{-5} mm³/h for the SS archwire. The total wear of the in vivo exposed NiTi and SS archwires is three- and four-times higher when compared to new wires, respectively.

The surface chemistry of new and in vivo exposed NiTi and SS archwires in the wear tracks and outside of the wear tracks were characterized by AES (Figure 5 for NiTi and Figure 6 for the SS archwires).

AES analysis of the new NiTi archwires showed the presence of titanium, oxygen and carbon on the surface, and AES sputter depth profiling showed that Ni and Ti increase beneath the surface oxide layer with an estimated thickness of the overlying thin oxide-passive film of 8 nm.

On a new NiTi archwire, in the wear track (Figure 5b), the analyzed spot was on a particulate with a very high O, Ca and Ti content. Only after 350 nm depth, the concentration of Ni started to increase. The analyzed spot is not an average representative of the oxide film in the wear track of a new NiTi archwire. Outside the wear track (Figure 5c), the estimated thickness is at 8 nm, similar to oxide film on a new NiTi. In the wear track of in vivo exposed NiTi archwire, a 14 nm thick layer contained

traces of S, constituent of saliva (Figure 5d). The layer outside the wear track (Figure 5e) in the in vivo exposed archwire is a mixture of Ti, Ni, O and C of organic origin as dental plaque. In our studies, the chemical composition of in vivo NiTi exposed dental plaque was characterized [23] by EDS and FTIR. A mineralogical analysis showed the presence of calcite, halite and sylvite on the surface of NiTi, on the surface of in vivo exposed SS apatite calcite and halite were found [23].

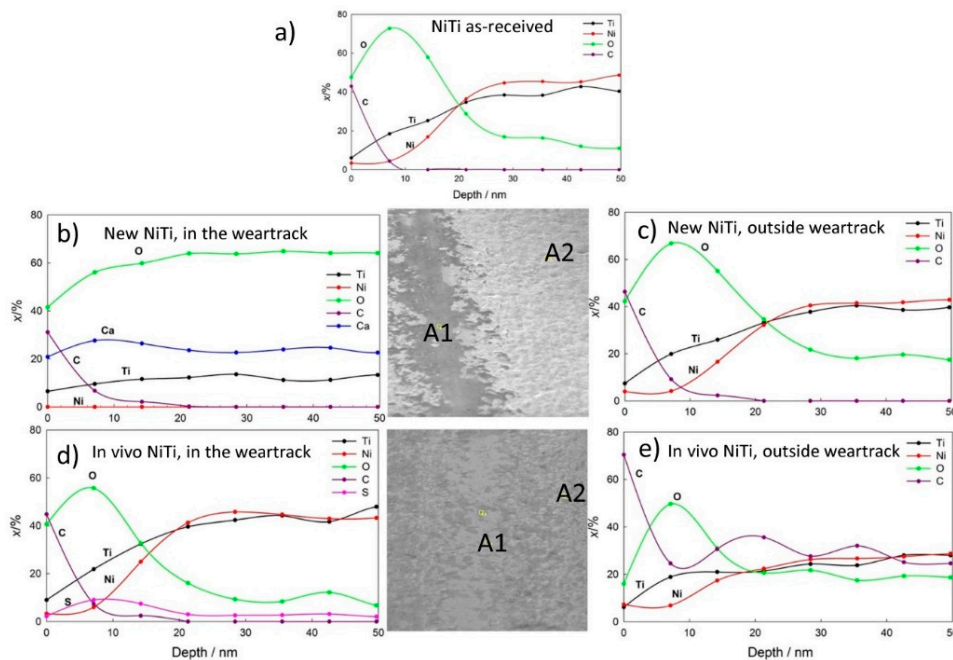


Figure 5. AES depth profiles for as-received NiTi archwire (a), NiTi new archwire in the wear track (b) and outside the wear track (c) and in vivo exposed NiTi archwire after the tribocorrosion experiment, in the wear track (d) and outside the wear track (e); A1 analysis in the weartrack; A2 analysis outside weartrack.

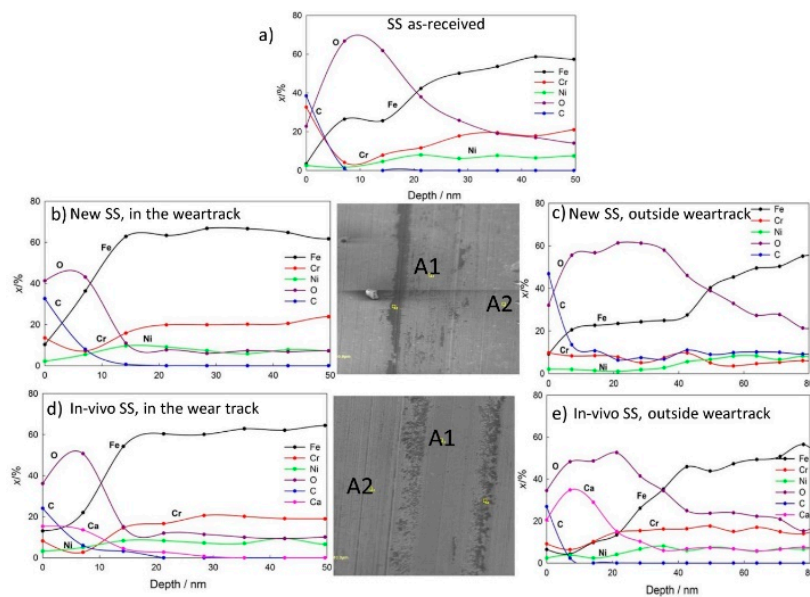


Figure 6. AES depth profiles for as-received SS archwire (a), SS new archwire in the wear track (b) and outside the wear track (c) and in vivo exposed SS archwire after tribocorrosion experiment, in the wear track (d) and outside the wear track (e); A1 analysis in the weartrack; A2 analysis outside weartrack.

AES depth profiles for SS archwires are presented in Figure 6.

AES depth profiling for as-received SS confirms the presence of a Cr_2O_3 oxide film. On the surface of the new SS and in vivo exposed SS after the tribocorrosion experiment (Figure 6c,e), thick layers of saliva deposits and dental plaque were found. The layers on the SS samples after the tribocorrosion experiments outside the wear tracks were 60–80 nm thick [24]. The oxide layer on SS in the wear track of a new wire (Figure 6b) is estimated at 1–2 nm, whereas in the case of in vivo exposed samples (Figure 6d), the outer part of the oxide film consists of C and Ca with O. It seems that the oral deposit is hard enough not to be fully removed by the 1 N force applied during tribocorrosive wear.

4. Discussion

Electrochemical investigation showed that in vivo exposed SS archwires with surface oxide film showed better corrosion properties than the new SS archwire. In the given environment, the measured susceptibility to local types of corrosion might result in the formation of small crevices when the SS archwire is in contact with stainless-steel brackets [35]. These crevices could cause early archwire breakdown.

Smaller passive currents in the anodic region, and a higher breakdown potential for both new and in vivo exposed NiTi archwires in comparison to SS archwires, indicate the lower susceptibility of NiTi archwires to corrosion due to the formation of a TiO_2 oxide layer, which better protects the NiTi archwires from the corrosion processes that occur in the presence of saliva. The in vivo exposed NiTi archwire and SS archwire exhibited better corrosion properties than the new archwires, mainly because of the protective nature of the film which was deposited on the surface of the archwires that was previously exposed in the patient's mouth.

Lowering of the potentials during sliding is in accordance with the results of previous studies, which reported lower open circuit potential when sliding [26,32]. The decrease in potential is greater when the normal load or when sliding velocity increases [26,32]. The re-passivation time for a new SS archwire was found to be longer than that for a new NiTi archwire, and this result could have an effect on the metal dissolution and oxide formation.

The tribo-electrochemical experiments and measurements of the coefficient of friction carried out in the study showed that this coefficient was higher for the NiTi archwires as a result of lower hardness. In the case of SS archwires, the coefficient of friction was smaller and caused smaller fluctuations in corrosion potential during mechanical wear in simulated saliva. Similar findings have been reported in the case of the tribological contact of NiTi with TiAlV and SS 316 alloy, where the coefficients of friction were higher for NiTi dental alloy (0.51 and 0.56, respectively), whereas in the case of the SS 304 alloy, the coefficients of friction were smaller (0.26 and 0.32, respectively) [36].

During the rubbing contact in corrosive saliva, the contribution of corrosion to the total wear is mainly due to the synergistic effects of wear. It was confirmed that the electrochemical contribution is minimal in the absence of wear. The total wear of the in vivo exposed NiTi and SS archwires was approximately four-times higher (Figure 4) when compared to the new archwires. The mechanical impact on the total wear of the in vivo exposed wires was higher in the case of the NiTi archwires (56%) when compared to the in vivo exposed SS archwires (32%). In general, corrosion wear was greater in the case of the new NiTi archwire than that of the new SS archwire. This could be the result of a thicker surface oxide film on the NiTi archwire, which is formed during wear and after it.

When exposed to air or biological liquids at body temperature, NiTi alloys, similar to AISI 304 L stainless steel, spontaneously form oxide passive layers. In the case of NiTi, a thin TiO_2 oxide passive film of 4–10 nm thickness forms, and in the case of SS, a thin Cr_2O_3 film of 1–2 nm thickness forms [24,33,34].

In general, the SS archwires had better mechanical characteristics than the NiTi archwires, which have shown better corrosion resistance that was found to be in agreement with the AES results. Wear of the in vivo exposed NiTi archwire was higher when compared to the new archwire due to the thicker oxide film, including the deposits (Figure 4). The estimated thickness of the TiO_2

passive film on as-received NiTi is 8 nm; on in vivo exposed NiTi archwire, a 60–80 nm thick organic film/dental plaque was observed. Faster repassivation times and the faster removal of oxide films during tribocorrosive wear accounts for possible higher ion migration, especially Ni, into the body of the patient, were reported elsewhere [13]. The wear rate of in vivo exposed SS archwires is higher due to removal of oxides and/or oral deposits.

The Cr₂O₃ passive film on as-received SS was 1–2 nm, while on in vivo exposed SS, the film was at about 60 nm.

From the presented study, it was found out that the main outcome for clinical scientists is that the amount of the accumulated plaque does not have any detrimental effect on orthodontic treatment. Coefficient of friction is higher for NiTi archwires than for SS archwires and is similar for new and in vivo exposed archwires. Thereby, saliva and debris do not have a clinical effect on the clinical outcome.

The main findings of the presented study for material scientists are the measured and evaluated differences between the NiTi and SS archwires concerning corrosion properties, wear properties and the amount and type of surface films on the new and in vivo exposed archwires.

However, the limitations of the presented study are especially in the number of studied specimens. For clinical relevance, usually a very high number of specimens is expected to define the properties reliably. Since in electrochemical investigations the main focus is on the characterization of the processes, a number of specimens is usually smaller. Due to this, our findings in clinical applications, where a wide range of parameters may be present, should be implemented with certain care.

5. Conclusions

Surface corrosion and wear properties of new and in vivo exposed nickel titanium (NiTi) and stainless-steel (SS) orthodontic archwires were evaluated. The following conclusions were drawn:

- AES surface analysis and depth profiling confirmed the formation of 8 nm thick TiO₂ films on new NiTi archwires. After tribocorrosion tests, the TiO₂ in the wear track was thinner. AES depth profiling showed up to 80 and 60 nm thick dental plaque on in vivo exposed NiTi and SS archwires, respectively. The passive film on new SS is mainly Cr₂O₃, with an estimated thickness of 1–2 nm.
- Electrochemical investigations showed that NiTi dental alloys exhibited better general corrosion properties compared to stainless-steel alloys, where susceptibility to local types of corrosion was detected. In vivo exposed NiTi and SS archwires showed better electrochemical properties in simulated saliva than new archwires.
- The total wear was lower for the new NiTi and SS wires when compared to in vivo exposed wires. When mechanical loads were used in corrosive saliva, corrosion was accelerated in both types of archwires. The contribution of mechanical wear to the total wear was higher for the new archwires when compared to the in vivo exposed archwires, where corrosion wear was found to be predominant.
- The coefficient of friction was higher in the NiTi archwires than in the SS archwires and is similar for new and in vivo exposed archwires. Thereby, saliva and debris do not have detrimental effect on the clinical outcome.

Author Contributions: Conceptualization, T.K., U.M., A.L. and J.P.; methodology, A.L.; validation, P.M., U.M., J.P. and T.K.; formal analysis P.M.; investigation, M.J.; writing—original draft preparation, T.K. and J.P.; writing—review and editing, T.K., M.J., A.L., M.O. and J.T.G.; supervision, M.O. All authors have read and agreed to the published version of the manuscript.

Funding: The work described in this paper was started within Grant No. L3-5501 and finalized within Grant No. L2-1831, both funded by the Slovenian Research Agency.

Acknowledgments: The help of Viljem Kuhar and Bojan Podgornik is gratefully acknowledged.

Conflicts of Interest: The authors declare no conflict of interest.

References

1. Araújo, R.C.; Bichara, L.M.; Araujoand, A.M.; Normando, D. Debris and friction of self-ligating and conventional orthodontic brackets after clinical use. *Angle Orthod.* **2015**, *85*, 673–677. [[CrossRef](#)]
2. Marques, I.S.; Araújo, A.M.; Gurgel, J.A.; Normando, D. Debris, roughness and friction of stainless steel archwires following clinical use. *Angle Orthod.* **2010**, *80*, 521–527. [[CrossRef](#)] [[PubMed](#)]
3. Kusy, R.P.; Whitley, J.Q. Resistance to sliding of orthodontic appliances in the dry and wet states: Influence of archwire alloy, interbracket distance, and bracket engagement. *J. Biomed. Mater. Res.* **2000**, *52*, 797–811. [[CrossRef](#)]
4. Schiff, N.; Dalard, F.; Lissac, M.; Morgon, L.; Grosogeat, B. Corrosion resistance of three orthodontic brackets: A comparative study of three fluoride mouthwashes. *Eur. J. Orthod.* **2005**, *27*, 541–549. [[CrossRef](#)] [[PubMed](#)]
5. House, K.; Sernettz, F.; Dymock, D.; Sandy, J.R.; Ireland, A.J. Corrosion of orthodontic appliances—should we care? *Am. J. Orthod. Dentofac. Orthop.* **2008**, *133*, 584–592. [[CrossRef](#)]
6. Mezeg, U.; Primožič, J. Influence of long-term in vivo exposure, debris accumulation and archwire material on friction force among different types of brackets and archwires couples. *Eur. J. Orthod.* **2017**, *39*, 673–679. [[CrossRef](#)]
7. Franchi, L.; Baccetti, T.; Camporesi, M.; Barbato, E. Forces released during sliding mechanics with passive self-ligating brackets or nonconventional elastomeric ligatures. *Am. J. Orthod. Dentofac. Orthop.* **2008**, *133*, 87–90. [[CrossRef](#)]
8. Huang, H.-H. Surface characterizations and corrosion resistance of nickel-titanium orthodontic archwires in artificial saliva of various degrees of acidity. *J. Biomed. Mater. Res. A* **2005**, *74A*, 629–639. [[CrossRef](#)]
9. Espinar, E.; Llamas, J.M.; Michiardi, A.; Ginebra, M.P.; Gil, F.J. Reduction of Ni release and improvement of the friction behaviour of NiTi orthodontic archwires by oxidation treatments. *J. Mater. Sci. Mater. Med.* **2011**, *22*, 1119–1125. [[CrossRef](#)]
10. Rincic Mlinaric, M.; Kanizaj, L.; Zuljevic, D.; Katic, V.; Spalj, S.; Otmacic Curkovic, H. Effect of oral antiseptics on the corrosion stability of nickel-titanium orthodontic alloys. *Mater. Corros.* **2018**, *69*, 510–518. [[CrossRef](#)]
11. Kuhta, M.; Pavlin, D.; Slaj, M.; Varga, S.; Laper-Varga, M.; Slaj, M. Type of Archwire and level of acidity: Effects on the release of Metal ions from Orthodontic appliances. *Angle Orthod.* **2009**, *79*, 102–110. [[CrossRef](#)] [[PubMed](#)]
12. Wichai, W.; Anuwongnukroh, N.; Dechkunakorn, S. Comparison of Chemical Properties and Ni Release of Stainless Steel and Nickel Titanium Wires. *Adv. Mater. Res.* **2014**, *884–885*, 560–565. [[CrossRef](#)]
13. Shabalovskaya, S.A. Biological aspects of TiNi alloy surfaces. *J. Phys. IV* **1995**, *5*, 1199–1204. [[CrossRef](#)]
14. Briceño, J.; Romeu, A.; Espinar, E.; Llamas, J.M.; Gil, F.J. Influence of the microstructure on electrochemical corrosion and nickel release in NiTi orthodontic archwires. *Mater. Sci. Eng. C* **2013**, *33*, 4989–4993. [[CrossRef](#)]
15. Močnik, P.; Kosec, T.; Kovač, J.; Bizjak, M. The effect of pH, fluoride and tribocorrosion on the surface properties of dental archwires. *Mat. Sci. Eng. C, Mat. Biol. Appl.* **2017**, *78*, 682–689. [[CrossRef](#)]
16. Milošev, I.; Kapun, B. The corrosion resistance of Nitinol alloy in simulated physiological solutions: Part 1: The effect of surface preparation. *Mat. Sci. Eng. C* **2012**, *32*, 1087–1096. [[CrossRef](#)]
17. Anuradha, P.; Varma, N.K.S.; Balakrishnan, A. Reliability performance of titanium sputter coated Ni–Ti arch wires: Mechanical performance and nickel release evaluation. *Biomed. Mater. Eng.* **2015**, *26*, 67–77. [[CrossRef](#)]
18. Undisz, A.; Schrepel, F.; Wesch, W.; Rettenmayr, M. Mechanism of oxide layer growth during annealing of NiTi. *J. Biomed. Mat. Res.* **2012**, *7*, 1743–1750. [[CrossRef](#)]
19. Makvandi, P.; Wang, C.-Y.; Nazarzadeh Zare, E.; Borzacchiello, A.; Niu, L.; Tay, F. Metal-based nanomaterials in biomedical applications: Antimicrobial activity and cytotoxicity aspects. *Adv. Funct. Mater.* **2020**. [[CrossRef](#)]
20. Zare, E.N.; Jamaledin, R.; Naserzadeh, P.; Afjeh-Dana, E.; Ashtari, B.; Hosseinzadeh, M.; Vecchione, R.; Wu, A.; Tay, F.R.; Borzacchiello, A.; et al. Metal-based Nanostructures/PLGA Nanocomposites: Antimicrobial Activity, Cytotoxicity and Their Biomedical Applications. *Appl. Mater. Interfaces* **2020**. [[CrossRef](#)]
21. Huang, H.H.; Chiu, Y.H.; Lee, T.H.; Wu, S.C.; Yang, H.W.; Su, K.H.; Hsu, C.C. Ion release from NiTi orthodontic wires in artificial saliva with various acidities. *Biomaterials* **2003**, *24*, 3585–3592. [[CrossRef](#)]
22. Wichelhaus, A.; Geserick, M.; Hibst, R.; Sander, F.G. The effect of surface treatment and clinical use on friction in NiTi orthodontic wires. *Dental Materials: Off. Publ. Acad. Dent. Mater.* **2005**, *21*, 938–945. [[CrossRef](#)] [[PubMed](#)]

23. Mezeg, U. Evaluation of Surface Properties of Orthodontic Brackets, Archwires and Their Degradation Processes in the Oral Cavity. Ph.D. Thesis, Medical Faculty at University of Ljubljana, Ljubljana, Slovenia, 2018.
24. Ovsenik, M.; Godec, M.; Kovač, J.; Dolinar, D.; Oblak, Č.; Kosec, T.; Jenko, M. Characterization of the surface chemistry and microstructure of new and in-vivo-exposed titanium-nickel shape-memory alloy and stainless steel AISI 304 archwires. In Proceedings of the 26th International Conference on Materials and Technology, Portorož, Slovenia, 3–5 October 2018; p. 105.
25. Mischler, S. Triboelectrochemical techniques and interpretation methods in tribocorrosion: A comparative evaluation. *Trib. Inter.* **2008**, *41*, 573–583. [[CrossRef](#)]
26. Celis, J.-P.; Ponthiaux, P.; Wenger, F. Tribo-corrosion of materials: Interplay between chemical, electrochemical and mechanical reactivity of surfaces. *Wear* **2006**, *261*, 939–946. [[CrossRef](#)]
27. Abedini, M.; Ghasemi, H.M.; Nili Ahmadabadi, M. Tribological behavior of NiTi alloy in martensitic and austenitic states. *Mat. Des.* **2009**, *30*, 4493–4497. [[CrossRef](#)]
28. Figueira, N.; Silva, T.M.; Carmezim, M.J.; Fernandes, J.C.S. Corrosion behaviour of NiTi alloy. *Electrochim. Acta* **2009**, *59*, 921–926. [[CrossRef](#)]
29. Duffo, G.S.; Castillo, Q. Development of artificial saliva solution for studying the corrosion behaviour of dental alloys. *Corrosion* **2004**, *60*, 594–602. [[CrossRef](#)]
30. Kosec, T.; Močnik, P.; Legat, A. The tribocorrosion behaviour of NiTi alloy. *App. Surf. Sci.* **2014**, *288*, 727–735. [[CrossRef](#)]
31. Tait, S.W. *An Introduction to Electrochemical Corrosion Testing for Practicing Engineers and Scientists*; PairODocs Publications: Racine, WI, USA, 1994.
32. Mathew, M.T.; Runa, M.J.; Laurent, M.; Jacobs, J.J.; Rocha, L.A.; Wimmer, M.A. Tribocorrosion behavior of CoCrMo alloy for hip prosthesis as a function of loads: A comparison between two testing systems. *Wear* **2011**, *271*, 1210–1219. [[CrossRef](#)]
33. Kocijan, A.; Donik, Č.; Jenko, M. Electrochemical and XPS studies of passive film formed on stainless steels in borate buffer and chloride solutions. *Corros. Sci.* **2007**, *49*, 2083–2098. [[CrossRef](#)]
34. Cumpson, P.J. The thickogram: a method for easy film thickness measurement in XPS. *Surf. Interface Anal.* **2000**, *29*, 403–406. [[CrossRef](#)]
35. Virtanen, S. Corrosion and passivity of metals and coatings. In *Tribocorrosion of Passive Metals and Coatings*, 1st ed.; Landolt, D., Mischler, S., Eds.; Woodhead Publishing in Materials: Cambridge, UK, 2011; pp. 3–28.
36. Alfonso, M.V.; Espina, E.; Llamas, J.M.; Rupérez de Gracia, E.; Manero Planella, J.M.; Barrera, J.M.; Solano, E.; Gil, M.; Javier, F. Friction coefficients and wear rates of different orthodontic archwires in artificial saliva. *J. Mat. Sci.: Mat. Med.* **2013**, *24*, 1327–1332. [[CrossRef](#)] [[PubMed](#)]



© 2020 by the authors. Licensee MDPI, Basel, Switzerland. This article is an open access article distributed under the terms and conditions of the Creative Commons Attribution (CC BY) license (<http://creativecommons.org/licenses/by/4.0/>).